High sensitivity SARS-CoV-2 detection using graphene oxide-multiplex qPCR

Yuanyuan Zeng [a],[1], Lili Zhou [b],[1], Zhongzhu Yang [a], Xiuzhong Yu [c], Zhen Song [a], Yang He [a],[*]

[a] *State Key Laboratory of Southwestern Chinese Medicine Resources, College of Medical Technology, Chengdu University of Traditional Chinese Medicine, Chengdu, Sichuan, 611137, China*
[b] *School of Laboratory Medicine, Chengdu Medical College, Chengdu, Sichuan, 610500, China*
[c] *Department of Laboratory Medicine, People's Hospital of Xinjin District, Chengdu, Sichuan, 611430, China*

HIGHLIGHTS

- A highly sensitive GO-multiplex qPCR method for SARS-CoV-2 detection.
- Adjust the GO oxidative degree to an appropriate sp^2 to sp^3 ratio.
- Construct the GO-forward primer composites to enhance assay sensitivity.
- GO-multiplex qPCR reduces the limit of detection to 10 copies/reaction.

GRAPHICAL ABSTRACT

ABSTRACT

The emerging pandemic of severe acute respiratory syndrome coronavirus 2 (SARS-CoV-2) critically challenges early and accurate virus diagnoses. However, the current gold standard for SARS-CoV-2 detection, reverse transcription-quantitative polymerase chain reaction (RT-qPCR), has reportedly failed to detect low-viral loads. One compound, graphene oxide (GO), which adsorbs single-stranded DNA (ssDNA), has been widely applied in molecular pathogen detection. This study presents a highly sensitive GO-multiplex qPCR method for simultaneous detection of two SARS-CoV-2 genes (*RdRP* and *E*) and one reference gene (*RNase P*). In a GO-multiplex qPCR system, GO pre-absorbs each forward primer to form specific GO-forward primer composites before entering the amplification system. Target gene amplification is confined within the primer-enriched composites, thus, improving the sensitivity of the assay. Compared to conventional multiplex qPCR, GO-multiplex qPCR reduces the limit of detection by 10-fold to 10 copies/reaction. Hence, the GO-multiplex qPCR assay can be effectively used for SARS-CoV-2 detection.

1. Introduction

The coronavirus disease 2019 (COVID-19) worldwide epidemic, caused by the highly infectious severe acute respiratory syndrome coronavirus 2 (SARS-CoV-2), has caused a critical global public health and economic crisis [1–3]. As of August 2022, over 600 million COVID-19 cases have been confirmed, more than 6 million deaths [4]. Pathogen SARS-CoV-2 is mainly transmitted through the respiratory tract, with extremely easy spread among populations, thus, causing aggregated infection [5]. Accurate detection is one of the basic requirements for screening SARS-CoV-2 infections.

Currently, reverse transcription-quantitative polymerase chain reaction (RT-qPCR) is considered the gold standard for SARS-CoV-2 detection [6]. Since the COVID-19 outbreak, the RT-qPCR testing capacity has dramatically increased worldwide, as millions of tests are performed daily. However, conventional RT-qPCR detects only 71% of SARS-CoV-2 infections, probably due to insufficient assay sensitivity and low sample concentrations caused by low-viral-load *in vivo* or improper clinical sampling [7,8]. Therefore, conventional RT-qPCR insufficiently supplies the clinical demand for screening SARS-CoV-2 infections and increases the potential risk of transmission. Multiplex qPCR is the commonly adopted assay for gene expression and single nucleotide polymorphism (SNP) analysis [9,10]. Multiplex qPCR detects different target genes simultaneously, although its application in clinical diagnosis is low due to the complexity of the system and possible interference between different amplification reactions. Consequently, a novel or improved high sensitivity multiplex qPCR system is necessary to enhance the accuracy of SARS-CoV-2 detection. Graphene oxide (GO) enhances the sensitivity of conventional PCR and single qPCR for detecting tuberculosis and ovarian cancer [11,12]. However, the application of GO to multiplex qPCR has not been reported. Since multiplex qPCR contains multiple pairs of primers, primer dimerization or mismatch hybridization are easily generated during the amplification process, resulting in lower amplification efficiency of the target product. In GO multiplex qPCR, the forward primers are pre-immobilized on the GO surface, and the forward primers will be released only when the target fragment is correctly paired with the primers, which will reduce the chance of primer mismatch and thus improve the sensitivity of GO-multiplex qPCR.

GO is an oxidation derivative of graphene, having a sp^2 region with a hexagonal honeycomb structure and the sp^3 carbon matrix region linked to oxygen-containing functional groups [13,14]. The sp^2 structural domain gives GO an affinity for aromatic rings and a fluorescence quenching ability. Moreover, the hydrophilic group attached to the sp^3 region stabilizes GO in aqueous solutions [15,16]. The large surface area, outstanding chemical functional groups, and unique interfacial properties give GO a strong ability to adsorb single-stranded DNA (ssDNA) [17]. Previous studies showed that GO adsorbs ssDNA through π-π stacking and hydrogen bonding [18,19]. Based on this property, more studies have demonstrated the excellent detection performance of GO-single PCR in disease diagnosis [20–22].

This study presents the first, highly sensitive GO-multiplex qPCR method for SARS-CoV-2 detection. The system employed the modified Hummers' method to prepare GO. The synthesis involved adjusting the GO oxidative degree to an appropriate sp^2 to sp^3 ratio. Then, the forward primers of the target genes were adsorbed by GO to construct the GO-forward primer composites. Fluorescence quenching and the shift in the UV absorption peak confirmed the formation of GO-forward primer composites. Besides, GO-forward primer composites significantly improved the sensitivity of multiplex qRT-PCR. Compared to conventional multiplex qRT-PCR, GO-multiplex qRT-PCR reduces the limit of SARS-CoV-2 detection by 10-fold.

2. Material and methods

2.1. Materials

Graphite (crystalline powder, 100 mesh) was purchased from Qingdao Laixi Colloidal Graphite Factory (Shandong, China). Potassium permanganate ($KMnO_4$), potassium nitrate (KNO_3), sulfuric acid (H_2SO_4), and 30% hydrogen peroxide (H_2O_2) were obtained from Chengdu Kelong Chemical Reagent Factory (Sichuan, China). The 3500 Da dialysis bag was purchased from Shanghai Yuanye Biological Science & Technology Company (Shanghai, China). Then, ultrapure water ($\geq$18 MΩ $\times$ cm resistivities at 25 °C) was used to prepare all aqueous solutions. All the reagents used in this study are analytical reagent grade.

2.2. Preparation of graphene oxide

Sulfuric acid (95%–98%) and carbon powder (0.5 g) were added to the beaker and mixed using a magnetic stirrer. Then, $KMnO_4$ (3 g) and $NaNO_3$ (0.5 g) were slowly added to the solution and stirred well to form dark green MnO_3^+. After settling under light-proof conditions, H_2O_2 (2.5 mL or 10 mL) was added to the embedded graphene for oxidation to form the GO stock solution. The residual acid and low molecular weight reaction products in the GO solutions were eliminated by dialysis in deionized water.

2.3. Characterization of graphene oxide

The FEI Tecnai G2 F30 S-TWIN transmission electron microscope (TEM) (FEI, OR, USA) was used for transmission electron microscopy. The atomic force microscopy (AFM) was obtained using the Bruker Dimension Icon Atomic force microscopy (Bruker Corporation, MA, USA). Raman scattering was performed using the Renishaw inVia microscope (Renishaw, England, UK). Then, the infrared spectra were obtained using the Fourier transform infrared spectroscopy (FT-IR) technique on the NICOLET IS10 FT-IR spectrometer (Thermo Fisher Scientific, MA, USA). The ultraviolet–visible (UV–vis) absorption spectra were measured using the MAPADA UV6300 UV–visible spectrophotometer (Mapada, Shanghai, China). The X-ray photoelectron spectroscopy (XPS) pattern of the samples was measured by a Thermo ESCALAB 250XI scanning XPS microscope (Thermo Fisher Scientific, MA, USA).

2.4. Establishing GO-forward primer composites

Primers and probes for *RdRP*, *E*, and *RNase P* genes were designed based on the methods of the World Health Organization (WHO) and the Centers for Disease Control and Prevention (CDC) [23,24]. For the multiplex test, the specific probes for *RdRP*, *E*, and *RNase P* genes were labeled with 4′,5′-dichloro-2′,7′-dimethoxy-6-carboxyfluorescein (JOE), carboxyrhodamine (ROX), and hexachlorofluorescein (HEX), respectively. Sangon Biotech (Shanghai, China) synthesized all the primers and probes (Table 1).

The GO stock solution was pre-sonicated for 20 min to make uniform

Table 1
Primers and probes used in this study.

Name	Oligonucleotide Sequence (5'>3')	Lable
RdRP_SARSr-F2	GTGARATGGTCATGTGTGGCGG	None
RdRP_SARSr-R1	CARATGTTAAASACACTATTAGCATA	None
RdRP_SARSr-P2	CAGGTGGAACCTCATCAGGAGATGC	5′JOE , 3′BHQ-1
E_Sarbeco_F1	ACAGGTACGTTAATAGTTAATAGCGT	None
E_Sarbeco_R2	ATATTGCAGCAGTACGCACACA	None
E_Sarbeco_P1	ACACTAGCCATCCTTACTGCGCTTCG	5′ROX , 3′BHQ-2
RNase P–F	AGATTTGGACCTGCGAGCG	None
RNase P –R	GAGCGGCTGTCTCCACAAGT	None
RNase P -P	TTCTGACCTGAAGGCTCTGCGCG	5′HEX , 3′BHQ-1

GO dilutions. Then, a one-to-one ratio of the GO dilution was mixed with 10 μM forward primers of *RdRP*, *E*, and *RNase P*. Next, the mixture was sonicated for 20 min and incubated on the thermostatic heater for 30 min to maximize primer adsorption on the GO surface. The effect of temperature on GO the adsorption capacity was investigated at 35 °C, 50 °C, 65 °C, and 80 °C, respectively. Finally, the mixture was centrifuged at 13,800 g for 1 h to remove the upper unbound GO layer. Instead of GO, RNase-free ddH$_2$O was used as a control group after processing at room temperature (25 °C) according to the above steps. The concentration of the forward primer in all three GO-forward primer composites was 5 μM.

2.5. Establishment of the GO-multiplex qPCR method

For GO-multiplex qPCR, the 25 μL reactions contained 12.5 μL Perfect Start™ II probe qPCR SuperMix (TransGen Biotech, Beijing, China), 0.5 μL each 10 μM probe, 1 μL each GO-forward primer composites, 0.5 μL each 10 μM reverse primer, 1 μL each DNA template, and 3.5 μL RNase-free ddH$_2$O. The conventional multiplex qPCR involved 25 μL reactions containing 12.5 μL Perfect Start™ II probe qPCR SuperMix (TransGen Biotech, Beijing, China), 0.5 μL each 10 μM probe, 0.5 μL each 10 μM forward primer, 0.5 μL each 10 μM reverse primer, 1 μL each DNA template, and 5 μL RNase-free ddH$_2$O. The concentration of the forward primers in the conventional multiplex qPCR and GO-multiplex qPCR systems are the same, both at 0.2 μM.

The GO-multiplex and conventional multiplex qPCRs were performed for 40 cycles on the qTOWER 2.2 fluorescent quantitative gradient thermocycler (Analytik Jena AG, Jena, Germany). Each cycle involved 94 °C of denaturation (30 s) followed by 40 cycles of 94 °C (5 s) and 60 °C (30 s). The reporter dyes were JOE (for *RdRP*), ROX (for *E*), and HEX (for *RNase P*). The negative control was RNase-free ddH$_2$O instead of the DNA template. Result with ≤37 Ct values were considered positive.

The GO stock solutions for GO-multiplex qPCR were diluted to 5.21, 7.45, 10.11, 13.44, 15.58, 19.12, 21.75, and 23.46 μg/mL. Different concentrations of GO dilutions were prepared as GO-forward primer composites of *RdRP*, *E*, and *RNase P* genes, respectively. Subsequently, the GO-forward primer composites of different genes were applied to the GO-multiplex qPCR. The optimum GO concentration was determined by comparing the Ct values of each gene with the conventional multiplex qPCR.

2.6. The specificity and sensitivity of GO-multiplex qPCR

The GO-multiplex qPCR specificity was evaluated using nine common respiratory viruses, including two RNA and seven DNA viruses. The two RNA viruses (coronavirus HKU1 and human parainfluenza virus) and seven DNA viruses (enterovirus, adenovirus, rhinovirus, human cytomegalovirus, varicella-zoster, mumps, and measles viruses) were obtained from Maccura Biotechnology (Sichuan, China). SARS-CoV-2 and the nine viruses were tested simultaneously using GO-multiplex and multiplex qPCR.

The sensitivity of the GO-multiplex qPCR method was determined using three plasmids containing *RdRP*, *E*, and *RNase P* target sequences. All plasmids were purchased from Sangon Biotech (Shanghai, China). Each plasmid template was serially diluted from 10^7 to 10^1 copies/μL. Thus, each plasmid concentration was simultaneously tested using the two methods to compare the sensitivities of GO-multiplex and conventional multiplex qPCR for SARS-CoV-2 detection.

2.7. Evaluation of the assay using SARS-CoV-2 pseudovirus

SARS-CoV-2 pseudoviruses containing *RdRP* and *E* target sequences were obtained from Maccura Biotechnology (Sichuan, China). SARS-CoV-2 RNA was extracted using the MagicPure® Simple Viral DNA/RNA Kit (TransGen Biotech, Beijing, China). Next, the RNA samples

were diluted into five different concentrations (10^5, 10^4, 10^3, 10^2, 10^1 copies/μL) and reverse transcribed using the TransScript® First-Strand cDNA Synthesis SuperMix Kit (TransGen Biotech, Beijing, China). Also, these samples were tested simultaneously to compare the performances of the GO-multiplex and multiplex qPCR techniques.

2.8. Adsorption efficiency of GO on ssDNA

The *RdRP*, *E*, and *RNase P* forward primers were labeled with JOE, ROX, and HEX fluorescent reporter dyes at the 5′ end, respectively (Sangon Biotech, Shanghai, China). These labeled primers were mixed separately with the optimized GO solution and water as the control. Then, the mixtures were divided into four portions and incubated at 35, 50, 65, and 80 °C for 30 min, respectively. The mixtures were covered with tin foil during incubation to avoid fluorescence decay. The fluorescence intensity of these mixtures was measured by using SpectraMax® iD5 (SelectScience, Bath, UK).

2.9. Validation of GO-forward primer composites

The GO-forward primer composites for *RdRP* gene were prepared as described above, with 5 μM of primer concentration. In addition, the forward primer for *RdRP* gene was diluted to 5 μM. The UV absorption peaks of the forward primer, GO-forward primer composites and GO dilution solution were obtained by Nano-500 (Allsheng, Hangzhou, China).

3. Results

3.1. Characterization of GO

A TEM was used to reveal the structural form of GO in 2.5 mL and 10 mL H$_2$O$_2$ (Fig. 1a and b). The GO prepared in 2.5 mL H$_2$O$_2$ contained an abundant and homogeneous sp^2 lattice. However, the GO prepared in 10 mL H$_2$O$_2$ had numerous disordered regions with few typical sp^2 lattices. Fig. 1c and d shows the morphology of GO samples visualized by AFM imaging. The average lateral GO size in 2.5 mL H$_2$O$_2$ was approximately 2 μm. Increasing the volume of H$_2$O$_2$ to 10 mL reduced the GO lateral size. The GO Raman spectra exhibited two prominent bands, 1374 cm^{-1}, and 1598 cm^{-1}, corresponding to D (sp^3-hybridized C) and G (sp^2-hybridized C) bands, respectively (Fig. 1e). FT-IR are illustrated in Fig. 1f, the GO spectrum in 2.5 mL H$_2$O$_2$ revealed characteristic absorption bands at 3419, 1734, 1626, 1279, and 1099 cm^{-1}, caused by O–H stretching vibration, C=O stretching vibration, C=C stretching vibration, epoxy C–O–C bending vibration, and C–O stretching vibration, respectively. Fig. 1g illustrated the XPS findings of GO, the deconvoluted C1s peak from each functional group were C=C (284.6 eV), C–C (285.7 eV), C–O (287.0 eV), C=O (288.0 eV), and O–C=O (289.0 eV). The carbon and oxygen contents were 63.36% and 33.57%, with a 1.89 carbon-oxygen ratio. The approximate sp^2-sp^3 ratio of GO prepared in 2.5 mL H$_2$O$_2$ was determined from the peak areas of different functional groups as 1:1 (Table S1). The UV–Vis spectroscopy of GO revealed that GO exhibited characteristic absorption peaks ascribed to the π-π* transition of C=C at 230 nm and n-π* transition of C=O at 295 nm (Fig. 1h).

3.2. Optimization of GO solutions

The ratio of sp^2 and sp^3 regions and the size of the GO-specific surface area affects its adsorption capacity. Therefore, the H$_2$O$_2$ volume (2.5 and 10 mL) was varied during GO preparation to adjust the ratio of sp^2 and sp^3 regions and the size of the specific surface area, facilitating the synthesis of GO with a high adsorption capacity. The characterization results of TEM, AFM, FT-IR, and Raman have confirmed that the GO prepared using 2.5 mL H$_2$O$_2$ has a larger specific surface area and a higher ratio of sp^2 region than GO prepared using 10 mL H$_2$O$_2$.
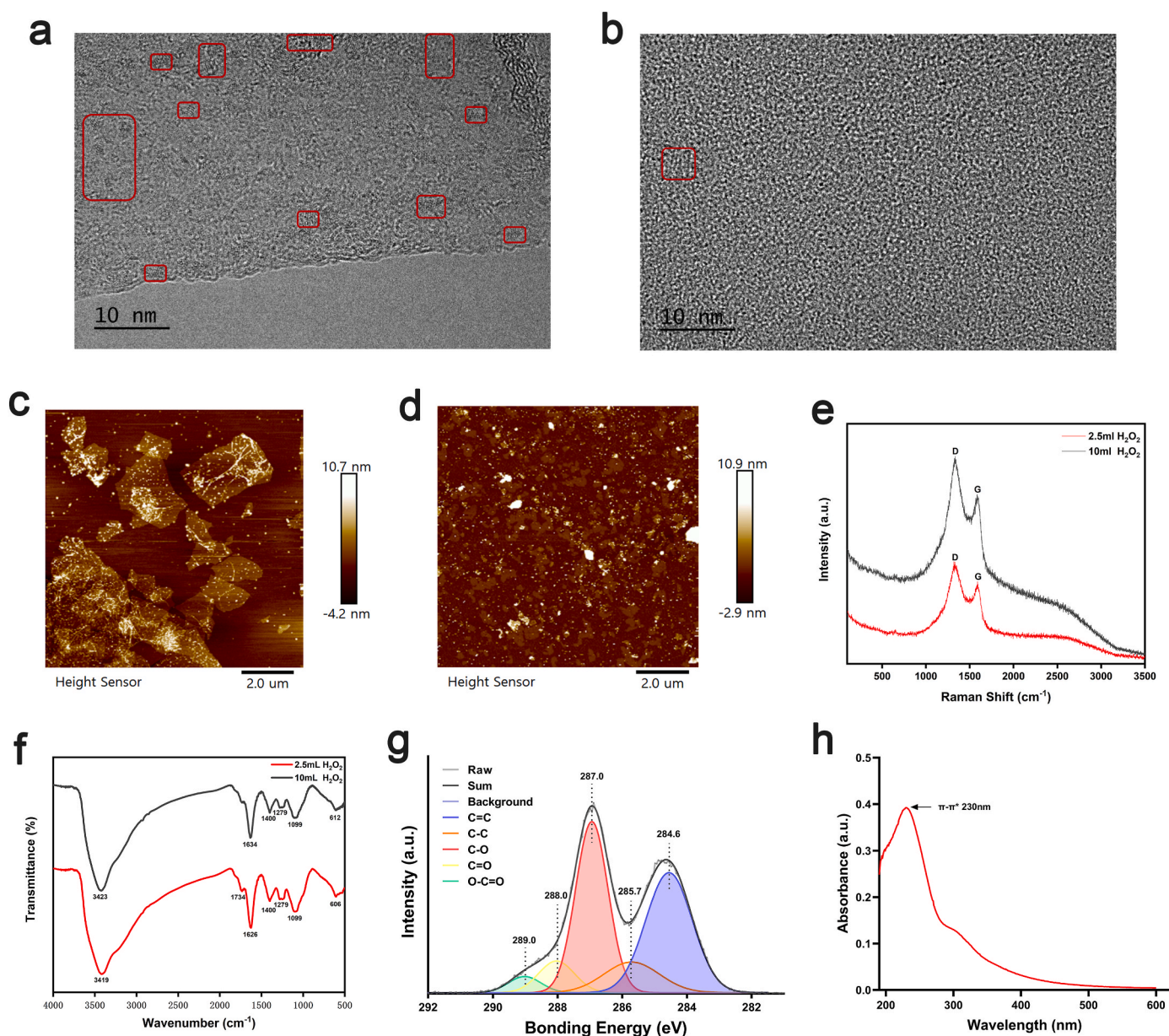
Fig. 1. Characterization of GO. TEM image of the GO prepared by 2.5 mL H_2O_2 (a) and by 10 mL H_2O_2 (b). AFM image of the GO prepared by 2.5 mL H_2O_2 (c) and by 10 mL H_2O_2 (d). (e) Raman spectra of the GO prepared by 2.5 and 10 mL H_2O_2. (f) FT-IR spectra of the GO prepared by 2.5 and 10 mL H_2O_2. (g) High-resolution XPS C1s spectra of the GO. (h) UV–vis absorption spectrum of the GO.

Therefore, GO prepared using 2.5 mL H_2O_2 has great primer adsorption ability. In addition, GO prepared using 2.5 mL H_2O_2 had significantly reduced Ct values. Unlike conventional multiplex qPCR, GO prepared by 2.5 mL H_2O_2 decreased the Ct values of *RdRP*, *E*, and *RNase P* by 1.02, 0.59, and 0.89, respectively. Nevertheless, amplification using GO prepared by 10 mL H_2O_2 increased the Ct values of the *E* gene by 0.17 while decreasing the Ct values of *RdRP* and *RNase P* by 0.64 and 0.33, respectively. (Fig. 2a). Hence, the specific surface area and sp^2 ratio positively affect the ability of GO to adsorb primers. Thus, the GO prepared using 2.5 mL H_2O_2 was used for subsequent experiments.

High GO concentration degrades dispersion and causes aggregation and adhesion of numerous sp^2 regions. Hence, the GO concentration was optimized by diluting to different concentrations and constructing GO-forward primer composites for *RdRP*, *E*, and *RNase P* genes. Next, GO-multiplex qPCR was performed to establish the optimum GO concentration. GO concentrations of 10.11 and 13.44 μg/mL resulted in significantly low Ct values across the three genes compared to the

conventional multiplex qPCR. The most significant decrease in Ct values was observed at 13.44 μg/mL. The Ct values of *RdRP*, *E*, and *RNase P* genes decreased by 2.13, 2.44, and 2.07, respectively (Fig. 2b). However, the Ct values of all three genes increased at other GO concentrations compared to 13.44 μg/mL. Therefore, 13.44 μg/mL was the optimal GO concentration for GO-multiplex qPCR.

3.3. Optimization of temperature for GO-forward primer composites

Since GO quenches the fluorescence via fluorescence resonance energy transfer, this study proposed attenuating the quenching effect using pre-constructed GO-forward primer composites. High temperatures abate the GO adsorption ability to ssDNA. Accordingly, this study optimized the incubation temperature of GO-forward primer composites for sufficient binding. At 35 °C, the GO-forward primer composites did not promote the three target genes amplification in the multiplex qPCR system. Subsequently, increasing the temperature to 50 °C promoted the
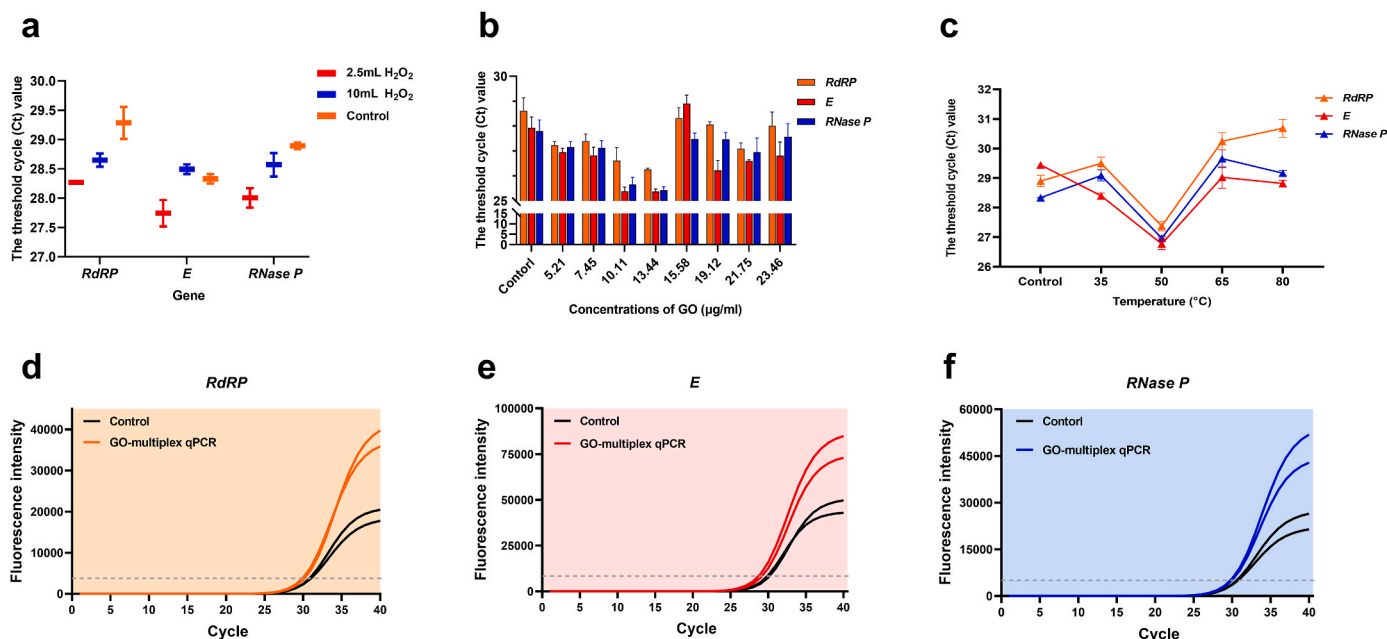
Fig. 2. Optimization of GO and GO-forward primer composites. (a) The effect of GO with different oxidation degree prepared by adjusting the volume of H_2O_2 on the multiplex-qPCR assay. (b) The effect of different concentrations of GO on the multiplex qPCR assay. (c) The effect of different incubation temperature of GO-forward primer composites on the multiplex qPCR assay. Amplification curves for (d) *RdRP*, (e) *E*, and (f) *RNase P* genes of GO-multiplex qPCR assay and conventional multiplex qPCR assays, respectively.

amplification of all target genes in multiplex qPCR. The Ct values of *RdRP*, *E*, and *RNase P* were reduced by 1.71, 2.64, and 1.34, respectively. Increasing the incubation temperature to 65 °C and 80 °C (or higher than 50 °C), increased the Ct values of *RdRP* and *RNase P* genes. Therefore, 50 °C was considered the optimum temperature for constructing GO-forward primer composites.

3.4. Specificity and sensitivity of the GO-multiplex qPCR

After optimization, the GO-forward primer composites were applied to subsequent GO-multiplex qPCR to assess the specificity of SARS-CoV-2 and nine other respiratory viruses. The GO-multiplex qPCR correctly discerned SARS-CoV-2 without any cross-reactivity (Fig. S1), demonstrating the high specificity of the GO-multiplex qPCR system established in this study.
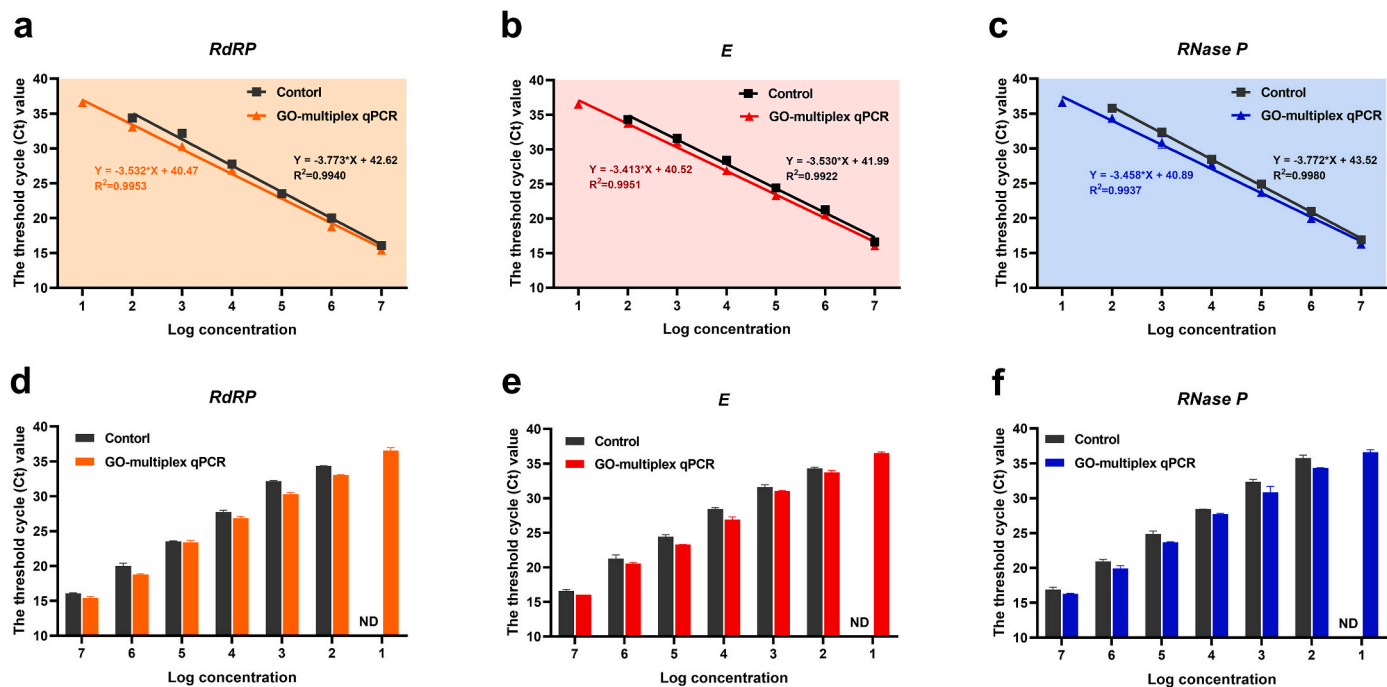
Fig. 3. Sensitivity analysis of the GO-multiplex qPCR method. Comparisons of standard curves for (a) *RdRP*, (b) *E*, and (c) *RNase P* between GO-multiplex qPCR method and conventional multiplex qPCR method. Comparisons of the Ct values of different concentrations of (a) *RdRP*, (b) *E*, and (c) *RNase P* plasmids detected by GO-multiplex qPCR method and conventional multiplex qPCR method.

Subsequently, GO-multiplex and conventional multiplex qPCR sensitivities were compared using 10-fold serial dilutions of the synthesized SARS-CoV-2 plasmids. Standard curves for *RdRP* (Fig. 3a), *E* (Fig. 3b), and *RNase P* (Fig. 3c) were obtained from GO-multiplex and conventional multiplex qPCR, respectively. The slopes of the GO-multiplex standard curves for the three genes were −3.532, −3.413, and −3.458, and their amplification efficiencies were 91.92, 96.33, and 94.62%, respectively. However, the slopes of conventional multiplex standard curves were −3.773, −3.530, and −3.772, and the amplification efficiencies were 84.09, 91.99, and 84.12%, respectively. A linear regression analysis of the standard curves showed that $R^2 > 0.99$. Furthermore, the Ct values from GO-multiplex qPCR were lower than conventional multiplex qPCR for the different concentrations. At 10 copies/μL, the probe signal was undetectable by conventional multiplex qPCR, while GO-multiplex qPCR detected *RdRP* (Fig. 3d), *E* (Fig. 3e), and *RNase P* (Fig. 3f) genes. Therefore, the limit of detection of GO-multiplex qPCR was 10 copies/reaction, which is 10-fold lower than conventional multiplex qPCR. These results indicate that GO-multiplex is more sensitive than conventional multiplex qPCR.

3.5. Evaluation of the assay using SARS-CoV-2 pseudovirus

The performance of GO-multiplex qPCR on real-life samples was evaluated by detecting pseudoviruses containing the SARS-CoV-2 partial genes. The viral RNA was extracted from the pseudoviruses and diluted to different viral loads for GO-multiplex qPCR analysis. Also, all the pseudovirus RNA samples were detected by conventional multiplex qPCR simultaneously to compare the GO-multiplex and conventional multiplex qPCR performances. As shown in Table 2, GO-multiplex qPCR correctly identified all the samples with different viral loads, and the Ct values were within the acceptable range (Ct < 37). In contrast, conventional multiplex qPCR did not effectively detect pseudoviruses in samples with low viral load. When GO-multiplex qPCR detected 10 copies/μL RNA, the Ct values of *RdRP* and *E* were undetectable and >37 in conventional multiplex qPCR, implying that conventional multiplex qPCR failed to detect low viral load (≤10 copies/μL RNA). Moreover, the Ct values of GO-multiplex qPCR profiled samples decreased compared to Ct values from conventional multiplex qPCR assays. Notably, the sensitivity of GO-multiplex qPCR for SARS-CoV-2 RNA was higher than conventional multiplex qPCR. These results demonstrate the potential of GO-multiplex qPCR for detecting low viral load in real-life samples.

3.6. Analysis and functionalization principles of the GO-forward primer composites

The mechanism and working principle of GO-multiplex qPCR is shown in Fig. 4a. The GO-forward primer composites are constructed and added directly to the multiplex amplification system. The SARS-CoV-2 nucleic acid fragments are attracted to the composite sheets and once the target genes are paired with the forward primers on the GO surface, the forward primers detach from it and carry out nucleic acid amplification.

To analyze the GO-forward primer composite, we evaluated the adsorption efficiency of GO on the forward primer by utilizing the property that GO has fluorescence quenching. Once GO adsorbs ssDNA, it quenches the fluorescent reporter group at the 5′ end of the ssDNA. Therefore, the fluorescence quenching efficiency before and after the coupling with GO reflects the adsorption efficiency of the primer. At temperatures below 50 °C, the fluorescence quenching efficiency of all three fluorescent reporter groups was <15%. However, at 50 °C, the GO surface adsorbed abundant primers with significantly increased fluorescence quenching efficiency for the three fluorescent reporter groups (JOE: 21.93%, ROX: 28.20%, and HEX: 22.89%) (Table S2). Subsequently, increasing the temperature decreased the fluorescence quenching efficiency. At 80 °C, the fluorescence quenching efficiency of the three groups was <15%, implying that the primers were not readily adsorbed to the GO surface (Fig. 4b). In addition, GO-multiplex qPCR showed that GO-forward primer composites prepared at 50 °C significantly reduced the Ct values of multiplex qPCR (Fig. 2c). Therefore, incubation at 50 °C maximizes the efficiency of GO adsorption to primers.

In addition, to demonstrate the fact that the forward primer coupled with GO, we analyzed the UV absorption peaks of the forward primer, GO and GO-forward primer composites separately. The results are shown in Fig. 4c, the maximum absorption peak of GO is at 230 nm. When the GO-forward primer composites were formed, the absorption peak was red-shifted (24 nm) and the maximum absorption peak appeared at 254 nm. This shift in wavelength is caused by GO and forward primers linked together by π–π stacking and hydrogen bonding. Thus, it was further confirmed that GO-forward primer composites were successfully constructed.

4. Discussion

In conventional multiplex qPCR, multiple pairs of primers and target genes fragments are mixed together in a PCR tube. Therefore, primer dimers or mismatch hybridization are more likely to form in conventional multiplex qPCR than single qPCR. However, dimerization and mismatch hybridization will consume reaction components and produce impaired rates of annealing and extension causing multiplex qPCR sensitivity to be decreased [25]. The elimination of dimerization and mismatch hybridization in nucleic acid amplification reactions using GO has been reported [26,27]. In addition, GO was proved to inhibit the formation of mismatched primer-template complexes in each PCR cycle [28]. However, most of these studies have focused on improving PCR specificity using GO. Considering that the current challenge for SARS-CoV-2 detection is mainly to accurately screen out low-viral-load samples [29,30], this study will focus on how to improve the sensitivity of multiplex qPCR for SARS-CoV-2 detection.

In previous studies, GO coupled with primers by simple incubation in single qPCR was effective in improving sensitivity [12]. This simple incubation pattern was applied to multiplex qPCR, i.e., the forward and reverse primers of *RdRP*, *E*, *RNase P* were added to the multiplex qPCR system for amplification after co-incubation with GO. The results showed that the GO-primer mixture had a significant inhibitory effect on the multiplex qPCR, and even the gene was not amplified (Fig. S2). We speculate that this result is due to the multiplex amplification system was introduced with excessive GO without primer binding, because free GO could not be separated from the effective GO-primer composites after a simple incubation process. When the three GO-primer mixtures are added to the multiplex amplification system at the same time, it is imperative that too much unbound GO is introduced. As a result, the free GO may stick in the system and will affect the release of the target product. Therefore, we reduced this effect by increasing the steps of

Table 2
Comparative results of SARS-CoV-2 pseudovirus detection using GO-multiplex qPCR method and conventional multiplex qPCR method.

RNA concentration (copies/μL)	GO-multiplex qPCR		Conventional multiplex qPCR	
	RdRP	E	RdRP	E
10	36.52/ 36.92	36.43/ 36.99	ND	37.29/ 38.65
10^2	34.27/ 34.20	33.03/ 33.29	35.75/ 35.88	33.85/ 33.57
10^3	30.49/ 30.96	30.29/ 30.40	32.43/ 32.69	31.74/ 31.43
10^4	27.22/ 27.61	26.07/ 26.52	28.36/ 28.13	27.64/ 27.99
10^5	22.95/ 23.12	22.71/ 22.52	24.21/ 24.12	24.09/ 23.43

ND: Not Detected.
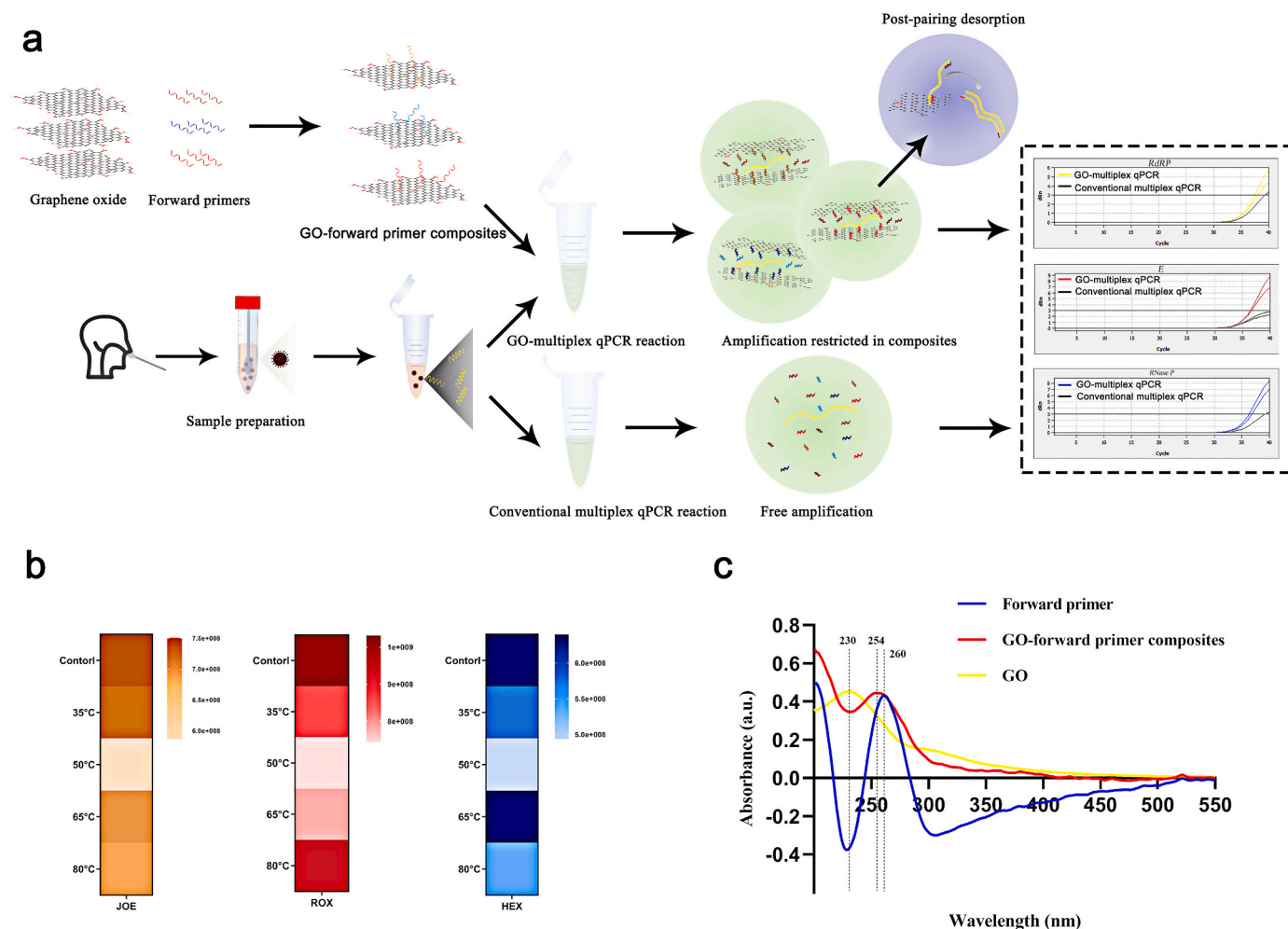
Fig. 4. The mechanism of GO-forward primer composites to improve the sensitivity for multiplex qPCR. (a) Graphical representation of the working principle of GO-forward primer composites in multiplex qPCR. (b) Fluorescence intensity of ssDNA after adsorption by GO at different incubation temperatures. (c) UV–vis absorption spectrum of the GO, GO-forward primer composites and forward primer.

sonication and centrifugation to remove the unbound primers GO, thus improving the sensitivity of multiplex qPCR for the three target genes of SARS-CoV-2.

GO have ability to adsorb ssDNA by π–π stacking interaction and hydrogen bonding. The 5′ ends of three forward primers used in the experiment were labeled by fluorescent groups and then coupled with GO. Since GO has a fluorescence quenching effect [31], the signal of the fluorescent group at the 5′ end of the primer will be quenched when it is adsorbed by GO. Thus, we confirmed that all three forward primers were successfully adsorbed by GO. Furthermore, we investigated the adsorption capacity of GO at different incubation temperatures. The results showed that the strongest fluorescence quenching efficiency and the most significant reduction in the Ct value of GO-multiple qPCR were observed when the incubation temperature at 50 °C. On the other hand, the red-shift of the UV absorption peak (24 nm) also confirms that the forward primers are indeed adsorbed by GO and form the GO-forward primer composites.

The presence of the GO-forward primer composites in the amplification system attracted the free single-stranded templates and reverse primers to the different composite lamellae. The template had successfully paired with the primers to form the double-stranded structure before annealing. Since GO has a low affinity for double-stranded DNA, the forward primers on the GO surface are released and confined to the amplification space between GO sheets. This pattern increases the chance of primer-template collisions, making it easier to form

amplicons. In addition, GO has excellent thermal conductivity, shortening the thermal response time of the reaction components in GO-multiplex qPCR cycles. The above mechanism shows that GO-forward primer composites can effectively improve the sensitivity of multiplex qPCR. The sensitivity of the GO-multiplex qPCR method for detecting SARS-CoV-2 was evaluated using standard plasmids of *RdRP, E*, and *RNase P* genes. Compared with the conventional method, the GO-multiplex qPCR method improved the amplification efficiency of the three target genes simultaneously (*RdRP*: 7.83%, *E*: 4.34%, *RNase P*: 10.50%). In addition, validations using the SARS-CoV-2 pseudovirus showed that the GO-multiplex exhibits higher sensitivity in detecting RNA templates than the conventional multiplex qPCR method.

5. Conclusion

In summary, this study developed a GO-multiplex qPCR method for detecting SARS-CoV-2. In a GO-multiplex qPCR, GO can enrich the primers on the surface and significantly improve the sensitivity of SARS-CoV-2 detection. The GO-multiplex qPCR limit of detection is 10 copies/reaction, 10-fold lower than conventional multiplex qPCR. Besides, GO has non-specific ssDNA adsorption, a powerful tool for enhancing the fight against the COVID-19 pandemic and rapid detection of other pathogens.

CRediT authorship contribution statement

Yuanyuan Zeng: Methodology, Investigation, Writing – original draft, Writing – review & editing. **Lili Zhou:** Methodology, Investigation, Writing – original draft, Writing – review & editing. **Zhongzhu Yang:** Investigation, Characterization analysis. **Xiuzhong Yu:** Investigation, Writing – review & editing. **Zhen Song:** Formal analysis. **Yang He:** Conceptualization, Funding acquisition, Investigation, Supervision, Writing – review & editing.

Declaration of competing interest

The authors declare that they have no known competing financial interests or personal relationships that could have appeared to influence the work reported in this paper.

Data availability

No data was used for the research described in the article.

Acknowledgements

Appendix A. Supplementary data

Supplementary data to this article can be found online at https://doi.org/10.1016/j.aca.2022.340533.

References

[1] H.M. Ashour, W.F. Elkhatib, M.M. Rahman, H.A. Elshabrawy, Insights into the recent 2019 novel coronavirus (Sars-coV-2) in light of past human coronavirus outbreaks, Pathogens 9 (2020) 1–15, https://doi.org/10.3390/pathogens9030186.

[2] W.J. Wiersinga, A. Rhodes, A.C. Cheng, S.J. Peacock, H.C. Prescott, Pathophysiology, transmission, diagnosis, and treatment of coronavirus disease 2019 (COVID-19): a review, JAMA, J. Am. Med. Assoc. 324 (2020) 782–793, https://doi.org/10.1001/jama.2020.12839.

[3] M. Nicola, Z. Alsafi, C. Sohrabi, A. Kerwan, A. Al-Jabir, C. Iosifidis, M. Agha, R. Agha, The socio-economic implications of the coronavirus pandemic (COVID-19): a review, Int. J. Surg. 78 (2020) 185–193, https://doi.org/10.1016/j.ijsu.2020.04.018.

[4] World Health Organization, WHO Coronavirus (COVID-19) Dashboard. https://covid19.who.int/.

[5] E.A. Meyerowitz, A. Richterman, R.T. Gandhi, P.E. Sax, Transmission of sars-cov-2: a review of viral, host, and environmental factors, Ann. Intern. Med. 174 (2021) 69–79, https://doi.org/10.7326/M20-5008.

[6] World Health Organization. Laboratory Testing of 2019 Novel Coronavirus (2019-nCoV) in Suspected Human Cases: Interim Guidance, World Health Organization, 17 January 2020. https://www.who.int/publications/i/item/laboratory-testing-of-2019-novel-coronavirus-(-2019-ncov)-in-suspected-human-cases-interim-guidance-17-january-2020.

[7] J.W. Fang Y, H. Zhang, J. Xie, M. Lin, L. Ying, P. Pang, Sensitivity of chest CT for COVID-19 comparison to RT-PCR, Lancet 296 (2020), https://doi.org/10.1148/radiol.2020200432. E115–E117.

[8] R. Rahbari, N. Moradi, M. Abdi, rRT-PCR for SARS-CoV-2: analytical considerations, Clin. Chim. Acta 516 (2021) 1–7, https://doi.org/10.1016/j.cca.2021.01.011.

[9] D. Khodakov, J. Li, J.X. Zhang, D.Y. Zhang, Highly multiplexed rapid DNA detection with single-nucleotide specificity via convective PCR in a portable device, Nat. Biomed. Eng. 5 (2021) 702–712, https://doi.org/10.1038/s41551-021-00755-4.

[10] A. Babiker, K. Immergluck, S.D. Stampfer, A. Rao, L. Bassit, M. Su, V. Nguyen, V. Stittleburg, J.M. Ingersoll, H.L. Bradley, M. Mavigner, N. Schoof, C.S. Kraft, A. Chahroudi, R.F. Schinazi, G.S. Martin, A. Piantadosi, W.A. Lam, J.J. Waggoner, Single-amplicon multiplex real-time reverse transcription-pcr with tiled probes to detect sars-cov-2 spike mutations associated with variants of concern, J. Clin. Microbiol. 59 (2021) 1–12, https://doi.org/10.1128/JCM.01446-21.

[11] A. Javed, S.R. Abbas, M.U. Hashmi, N.U.A. Babar, I. Hussain, Graphene oxide based electrochemical genosensor for label free detection of mycobacterium tuberculosis from raw clinical samples, Int. J. Nanomed. 16 (2021) 7339–7352, https://doi.org/10.2147/IJN.S326480.

[12] C. Hu, L. Zhang, Z. Yang, Z. Song, Q. Zhang, Y. He, Graphene oxide-based qRT-PCR assay enables the sensitive and specific detection of miRNAs for the screening of ovarian cancer, Anal. Chim. Acta 1174 (2021), 338715, https://doi.org/10.1016/j.aca.2021.338715.

[13] D.R. Dreyer, A.D. Todd, C.W. Bielawski, Harnessing the chemistry of graphene oxide, Chem. Soc. Rev. 43 (2014) 5288–5301, https://doi.org/10.1039/c4cs00060a.

[14] V. Georgakilas, J.N. Tiwari, K.C. Kemp, J.A. Perman, A.B. Bourlinos, K.S. Kim, R. Zboril, Noncovalent functionalization of graphene and graphene oxide for energy materials, biosensing, catalytic, and biomedical applications, Chem. Rev. 116 (2016) 5464–5519, https://doi.org/10.1021/acs.chemrev.5b00620.

[15] J. Kotakoski, Atomic and electronic structure of graphene, Graphene Prop. Prep. Charact. Appl. (2021) 15–26, https://doi.org/10.1016/B978-0-08-102848-3.00003-7. Second Ed.

[16] K.P. Loh, Q. Bao, G. Eda, M. Chhowalla, Graphene oxide as a chemically tunable platform for optical applications, Nat. Chem. 2 (2010) 1015–1024, https://doi.org/10.1038/nchem.907.

[17] B. Liu, S. Salgado, V. Maheshwari, J. Liu, DNA adsorbed on graphene and graphene oxide: fundamental interactions, desorption and applications, Curr. Opin. Colloid Interface Sci. 26 (2016) 41–49, https://doi.org/10.1016/j.cocis.2016.09.001.

[18] Z. Xu, X. Lei, Y. Tu, Z.J. Tan, B. Song, H. Fang, Dynamic cooperation of hydrogen binding and π stacking in ssDNA adsorption on graphene oxide, Chem. Eur J. 23 (2017) 13100–13104, https://doi.org/10.1002/chem.201701733.

[19] J. Lee, J. Kim, S. Kim, D.H. Min, Biosensors based on graphene oxide and its biomedical application, Adv. Drug Deliv. Rev. 105 (2016) 275–287, https://doi.org/10.1016/j.addr.2016.06.001.

[20] W. Guo, G. Xu, Y. Wang, Y. Nan, C. Wu, E.M. Zhou, Fluorescence resonance energy transfer combined with asymmetric PCR for broad and sensitive detection of porcine reproductive and respiratory syndrome virus 2, J. Virol. Methods. 272 (2019), 113710, https://doi.org/10.1016/j.jviromet.2019.113710.

[21] Z. Huang, Z. Luo, J. Chen, Y. Xu, Y. Duan, A facile, label-free, and universal biosensor platform based on target-induced graphene oxide constrained DNA dissociation coupling with improved strand displacement amplification, ACS Sens. 3 (2018) 2423–2431, https://doi.org/10.1021/acssensors.8b00935.

[22] S. Jeong, D.M. Kim, S.Y. An, D.H. Kim, D.E. Kim, Fluorometric detection of influenza viral RNA using graphene oxide, Anal. Biochem. 561–562 (2018) 66–69, https://doi.org/10.1016/j.ab.2018.09.015.

[23] World Health Organization, Diagnostic detection of 2019-nCoV by real-time RT-PCR. https://www.who.int/docs/default-source/coronaviruse/protocol-v2-1.pdf?sfvrsn=a9ef618c_2.

[24] Centers For Disease Control And Prevention, Research Use Only 2019-Novel Coronavirus (2019-nCoV) Real-time RT-PCR Primers and Probes. https://www.cdc.gov/coronavirus/2019-ncov/lab/rt-pcr-panel-primer-probes.html.

[25] P. Markoulatos, N. Siafakas, M. Moncany, Multiplex polymerase chain reaction: a practical approach, J. Clin. Lab. Anal. 16 (2002) 47–51, https://doi.org/10.1002/jcla.2058.

[26] S. Li, Y. Gu, Y. Lyu, Y. Jiang, P. Liu, Integrated graphene oxide purification-lateral flow test strips (iGOP-LFTS) for direct detection of PCR products with enhanced sensitivity and specificitfile, Anal. Chem. 89 (2017) 12137–12144, https://doi.org/10.1021/acs.analchem.7b02769.

[27] Y. Wang, W. wei Jiao, Y. Wang, Y. cui Wang, C. Shen, H. Qi, A.D. Shen, Graphene oxide and self-avoiding molecular recognition systems-assisted recombinase polymerase amplification coupled with lateral flow bioassay for nucleic acid detection, Microchim. Acta 187 (2020), https://doi.org/10.1007/s00604-020-04637-5.

[28] Y. Wang, F. Wang, H. Wang, M. Song, Graphene oxide enhances the specificity of the polymerase chain reaction by modifying primer-template matching, Sci. Rep. 7 (2017) 1–10, https://doi.org/10.1038/s41598-017-16836-x.

[29] A.A. Osman, M.M. Al Daajani, A.J. Alsahafi, Re-positive coronavirus disease 2019 PCR test: could it be a reinfection? New Microbes New Infect 37 (2020) 1–6, https://doi.org/10.1016/j.nmni.2020.100748.

[30] Y. Yan, L. Chang, L. Wang, Laboratory testing of SARS-CoV, MERS-CoV, and SARS-CoV-2 (2019-nCoV): current status, challenges, and countermeasures, Rev. Med. Virol. 30 (2020) 1–14, https://doi.org/10.1002/rmv.2106.

[31] Z. Liu, B. Liu, J. Ding, J. Liu, Fluorescent sensors using DNA-functionalized graphene oxide, Anal. Bioanal. Chem. 406 (2014) 6885–6902, https://doi.org/10.1007/s00216-014-7888-3.